Braz J Phys (2016) 46:133–142
DOI 10.1007/s13538-015-0377-0

SOCIEDADE BRASILEIRA DE FÍSICA

NUCLEAR PHYSICS

Role of Barrier Modification and Inelastic Surface Excitations in Sub-Barrier Fusion of $_{16}^{32}S+_{40}^{94}Zr$ Reaction

Manjeet Singh Gautam[1] · **Rajni**[1] · **Manoj K. Sharma**[1]

Received: 6 August 2015 / Published online: 7 January 2016

Abstract The fusion dynamics of $^{32}_{16}S+^{94}_{40}Zr$ reaction at near and sub-barrier energies is investigated within the context of different theoretical approaches. The various theoretical models like one-dimensional Wong formula, ℓ-summed extended Wong formula, the energy-dependent Woods-Saxon potential model (EDWSP model), and coupled channel formulation have been used to address the impacts of nuclear structure degrees of freedom of the colliding pairs. The roles of different Skyrme forces along with Wong formalism are also tested in the analysis of the sub-barrier fusion dynamics of the $^{32}_{16}S+^{94}_{40}Zr$ reaction. The influence of the low-lying surface vibrational states of the collision partners is investigated within the framework of coupled channel calculations performed by the code CCFULL. In the present work, it has been observed that the EDWSP model introduces barrier modification effects somewhat similar to those of the coupled channel approach, as well as those of using different Skyrme forces and hence it reasonably addresses the observed fusion data of $^{32}_{16}S+^{94}_{40}Zr$ reaction in the close vicinity of the Coulomb barrier.

Keywords Depth and diffuseness · Woods-Saxon potential · Heavy-ion collision · Sub-barrier fusion reactions · Coupled channel approach · Skyrme forces

✉ Manjeet Singh Gautam
gautammanjeet@gmail.com

[1] School of Physics and Material Science, Thapar University, Patiala, Punjab 147004, India

1 Introduction

The dynamics of heavy-ion fusion reactions near and below the Coulomb barrier has received considerable attention during the past few decades, on the theoretical as well as on the experimental front. The considerable interest behind the exploration of these reactions is to understand the nature of nuclear structure and the related interaction of the collision partners and subsequent compound system. In the fusion process, a projectile enters into the vicinity of target nucleus to form a compound nucleus, either by overcoming the Coulomb repulsion or via quantum mechanical tunneling through the potential barrier. Theoretically, the simplest way to address the fusion dynamics is through the barrier penetration model (BPM), wherein the collision partners are assumed to penetrate through their fusion barrier and form a composite system [1]. However, during last few decades, an anomalously large fusion enhancement at sub-barrier energies over the predictions of one-dimensional barrier penetration models has been observed in many projectile-target combinations. In general, this fusion enhancement has an intimate link with the coupling of the relative motion of reactants with the internal structure of the colliding nuclei, such as nuclear shape deformation, inelastic surface vibrations, rotations of nuclei during collision, neck formation, and nucleon transfer reactions. Strictly speaking, such couplings will produce substantially large enhancement in the fusion cross section at sub-barrier energies [2–5]. Although it is very difficult to take into account all intrinsic degrees of freedom simultaneously, an extensive effort has been made to include some of them so that the complex behavior of the fusion dynamics may be understood adequately. The relation between sub-barrier fusion enhancement and intrinsic degrees of freedom such as permanent shape deformation and low-lying surface vibrations of the fusing nuclei has been well established by the various coupled channel formulations [1–6]. However, the interplay of neutron transfer channels has not been fully understood because

the transfer of neutrons is insensitive to the fusion barrier and such transfer process starts at large internuclear separation between the reactants [7–11].

For a complete description of the fusion dynamics, the knowledge of nucleus-nucleus potential which consists of the Coulomb repulsive interaction, the centrifugal term, and the attractive short-range nuclear potential, is extensively important. The dynamics of nuclear reactions like elastic scattering, inelastic scattering, fusion reactions, or other reaction channels are extremely sensitive to the shape of nucleus-nucleus potential. Therefore, different parameterization of nuclear potential are most widely used to explain the various nuclear phenomena, and hence, many attempts have been made to extract information regarding the optimum form of nuclear potential by analyzing a large set of experimental data [12–15]. Generally, the fusion process is explained by using the three-parametric Woods-Saxon potential, namely the depth, the range, and the diffuseness, prove extremely sensitive ingredients of the nuclear interactions. The diffuseness parameter is directly related with the slope of the nuclear potential in the tail region of the Coulomb barrier, where the fusion starts to take place. Significantly large values of the diffuseness parameter (0.75 to 1.5 fm) have been used to explore the sub-barrier fusion data, while a much smaller value (0.65 fm) is generally used to explain the systematics of elastic scattering data [1, 7–10, 16]. This diffuseness anomaly is one of the challenging issues of heavy-ion fusion reaction, and the cause of such diffuseness anomaly is not understand completely. Therefore, it is still not clear why the Woods-Saxon form of the nuclear potential behaves differently in the elastic scattering process and in the fusion process. Hence, more intensive investigations are required to address this issue. In this regard, several attempts have been made to understand the cause of the diffuseness anomaly as well as the systematic failure of the static Woods-Saxon potential by introducing the energy dependence in the real part of nuclear potential in such a way that it becomes more attractive at sub-barrier energies [17–21]. This energy dependence in the nucleus-nucleus potential in turn induces closely similar physical effects that arise due to the coupling between the relative motion and the internal degrees of freedom of the colliding pairs. The energy dependence in the nucleus-nucleus potential arises from the nucleon-nucleon interaction as well as the non-local quantum effects [22]. The microscopic time-dependent Hartree-Fock theory provides theoretical support to the energy dependence of nucleus-nucleus potential which is originated from the various channel coupling effects [23]. Therefore, the energy-dependent nucleus-nucleus potential may provide better descriptions of the various dynamical aspects related with the fusion dynamics in the close vicinity of the Coulomb barrier. Therefore, it is reasonable to test the applicability of the energy-dependent nucleus-nucleus potential for the description of the sub-barrier fusion dynamics. Following this idea, the energy-dependent Woods-Saxon potential model (EDWSP model) was introduced, wherein the energy dependence in the Woods-Saxon potential was taken via its diffuseness parameter [17–21].

The rich interplay of inelastic surface excitations of the collision partners and neutron transfer channels attracted theoreticians to address the fusion dynamics of a variety of colliding partners. Zhang et al. [10] analyzed the fusion of the $^{32,36}_{16}S+^{90,96}_{40}Zr$ systems within the context of coupled channel formulation and suggested that there exist strong octupole vibrations in the $^{96}_{40}Zr$ nucleus. Furthermore, the significantly larger fusion enhancement of the $^{32}_{16}S+^{96}_{40}Zr$ system in comparison to other $S+Zr$ combinations arises due to the combined effects of strong octupole vibrations in the target and neutron transfer channels. Jia et al. [11] also discussed the fusion dynamics of $S+Zr$ combinations within the framework of coupled channel model and suggested that the inclusion of inelastic surface excitations alone could not explain the sub-barrier fusion data of the $^{32}_{16}S+^{94,96}_{40}Zr$ systems. To resolve the puzzling features of the fusion dynamics of the $^{32}_{16}S+^{94}_{40}Zr$ system, this work compares the predictions of different theoretical methods. The static Woods-Saxon potential in conjunction with one-dimensional Wong formula [24] fails to explain the fusion dynamics of this system, while the predictions of the EDWSP model [17–21] successfully explain the observed fusion dynamics of $^{32}_{16}S+^{94}_{40}Zr$ system. In addition, the role of different Skyrme interactions such as SIII and GSkI within the context of one-dimensional Wong and ℓ-summed extended Wong formula [25–28] is also tested for the description of the observed sub-barrier fusion enhancement of $^{32}_{16}S+^{94}_{40}Zr$ system. The nuclear potential obtained by using the Skyrme energy density formalism (SEDF) opens up the possibilities of using of variety of Skyrme forces which in turn introduce the different barrier characteristics, and hence, the barrier modification effects get introduced in the theoretical calculations. The barrier modification effects in sub-barrier fusion process depend critically on the choice of Skyrme force along with usual dependence on the type of nuclear reaction under consideration. The old SIII force [29–36] is weakly sensitive to neutron-proton asymmetry and isospin effects, while the newly parameterized GSkI force [37], which contains the tensor coupling with the spin and gradient components, includes the appropriate isospin effects as well as the density-dependent interactions. The theoretical predictions of the one-dimensional Wong formula using the SIII force strongly underestimate the experimental data, while the GSkI force could adequately describe the fusion excitation data in the sub-barrier region. However, at above barrier energies, the GSkI-based fusion cross section overestimates the experimental data. Therefore, the ℓ-summed extended Wong formula is applied, which takes care of overestimation of theoretical results at above barrier energies and consequently adequately describes the sub-barrier fusion enhancement of the $^{32}_{16}S+^{94}_{40}Zr$ system [25–28].

To account for the effects of inelastic surface vibrational states of the colliding pairs, coupled channel calculations for the $^{32}_{16}S+^{94}_{40}Zr$ system are performed using the code CCFULL [38]. The couplings to low-lying surface vibrational states of the reactants fail to reproduce the experimental data at sub-barrier energies. The large discrepancies between such

calculations and the data at sub-barrier energies arise due to existence of neutron pickup channels with positive ground state Q values. Furthermore, the coupled channel formulation predicted that in addition to inelastic surface excitations of the reactants, more intrinsic channels are needed for the complete description of the fusion dynamics of the $^{32}_{16}S+^{94}_{40}Zr$ system. The comparison of the theoretical predictions based upon the different theoretical models like EDWSP model and Skyrme interactions within energy density formalism, coupled channel formulation, reflects closely similar behavior of fusion dynamics of the $^{32}_{16}S+^{94}_{40}Zr$ system, and consequently, one can say that different approaches introduce similar kinds of barrier modification effects (barrier height, barrier position, and barrier curvature) in heavy-ion fusion reactions. A brief description of the method of calculation is given in Sect. 2. The results are discussed in Sect. 3, and the conclusions drawn are described in Sect. 4.

2 Theoretical Formalism

2.1 One-Dimensional Wong Formula

The fusion cross section within partial wave analysis is given by

$$\sigma_F = \frac{\pi}{k^2}\sum_{\ell=0}^{\infty}(2\ell+1)T_\ell^F \tag{1}$$

Based upon parabolic approximation of the effective interaction potential between colliding nuclei, Hill and Wheeler proposed following expression for tunneling probability (T_ℓ^F) [39]:

$$T_\ell^{\mathrm{HW}} = \frac{1}{1+\exp\left[\frac{2\pi}{\hbar\omega_\ell}(V_\ell - E)\right]} \tag{2}$$

The above Hill-Wheeler approximation was further simplified by Wong using the following assumptions for barrier position, barrier curvature, and barrier height [24]:

$$\begin{aligned} R_\ell &= R_{\ell=0} = R_B \\ \omega_\ell &= \omega_{\ell=0} = \omega \\ V_\ell &= V_{B0} + \frac{\hbar^2}{2\mu R_B^2}\left[\ell+\frac{1}{2}\right]^2 \end{aligned}$$

where V_{B0}, which is the sum of nuclear potential and Coulomb potential, corresponds to $\ell=0$ in the above expression. Using these assumptions and Eq. (2) into Eq. (1), the fusion cross section can be calculated as

$$\sigma_F = \frac{\pi}{k^2}\sum_{\ell=0}^{\infty}\frac{(2\ell+1)}{\left[1+\exp\frac{2\pi}{\hbar\omega}(V_\ell - E)\right]} \tag{3}$$

Since Wong assumes that infinite number of partial waves contribute to the fusion process, therefore, one can change the summation over ℓ into integral with respect to ℓ in Eq. (3), and by solving the integral, we get the following expression of Wong formula [24]:

$$\sigma_F = \frac{\hbar\omega R_B^2}{2E}\ell n\left[1+\exp\left(\frac{2\pi}{\hbar\omega}(E-V_{B0})\right)\right] \tag{4}$$

On integration over orientation angle θ_i and azimuthal angle Φ, the above fusion cross section becomes

$$\sigma_T = \int_{\theta_i,\Phi=0}^{\pi/2}\sigma_F \sin\theta_1 d\theta_1 \sin\theta_2 d\theta_2 d\Phi \tag{5}$$

The V_{B0} in Eq. (4) is the sum of nuclear potential and Coulomb potential, where the nuclear potential can be obtained by various approaches. In the present work, the theoretical calculations based upon Skyrme energy density formalism make the use of nuclear proximity potential (V_P) which will be discussed in Sect. 2.2, while the theoretical calculations based upon EDWSP model and coupled channel model make the use of Woods-Saxon form of nuclear potential which is discussed in Sects. 2.3 and 2.4. It is relevant to mention here that the total interaction potential is given by the following expression:

$$V_T(R) = V_P(R, A_i, \beta_{\lambda i}, T, \theta_i, \Phi) + V_C(R, Z_i, \beta_{\lambda i}, T, \theta_i, \Phi) + \frac{\ell(\ell+1)\hbar^2}{2\mu R^2} \tag{6}$$

where $\beta_{\lambda i}$, $\lambda=2,3,4$ are the static quadrupole, octupole, and hexadecapole deformations. In 2009, Gupta and collaborators [25] carried out the extension of Wong formula to include ℓ-summation explicitly in Eq. (1), which is known as ℓ-summed extended Wong formula, wherein the ℓ-summation is done up to $\ell_{\max}$, after including ℓ-summation up to $\ell_{\max}$, which is determined empirically for best fit to measure cross section and integrating over orientation angles to give total fusion cross section as by Eq. (5).

2.2 SEDF

The energy density formalism defines the nuclear interaction potential [26–28, 30–32] as

$$\mathrm{V}_P(R) = \mathrm{E}(R) - \mathrm{E}(\infty) \tag{7}$$

i.e., the nucleus-nucleus interaction potential as a function of separation distance, $\mathrm{V}_N(R)$, is the difference of the energy expectation value E of the colliding nuclei that are overlapping (at a finite separation distance R) and those that are completely separated (at $R=\infty$),where

$$\mathrm{E} = \int H\left(\vec{r}\right)d\vec{r} \tag{8}$$

with the energy density functional $H(r)$ consisting of kinetic, nuclear, and Coulomb interaction energy parts

$$H\left(\vec{r}\right) = \frac{\hbar^2}{2m}\left[\tau_p\left(\vec{r}\right) + \tau_n\left(\vec{r}\right)\right] + H_{\text{sky}}\left(\vec{r}\right) + H_{\text{coul}}\left(\vec{r}\right) \tag{9}$$

For the kinetic energy part, the extended Thomas-Fermi (ETF) approach including all terms up to second order in the spatial derivatives (ETF2) is applied [32]. The nuclear interaction part with Skyrme interaction $H_{\text{sky}}(r)$ [30–32, 40] is defined as

$$\begin{aligned} H_{\text{sky}}(r) &= \frac{1}{2}t_0\left[\left(1+\frac{1}{2}x_0\right)\rho^2 - \left(x_0+\frac{1}{2}\right)\left(\rho_p^2+\rho_n^2\right)\right] + \frac{1}{12}t_3\rho^\alpha\left[\left(1+\frac{1}{2}x_3\right)\rho^2 - \left(x_3+\frac{1}{2}\right)\left(\rho_p^2+\rho_n^2\right)\right] \\ &+ \frac{1}{4}\left[t_1\left(1+\frac{1}{2}x_1\right) + t_2\left(1+\frac{1}{2}x_2\right)\right]\tau\rho - \frac{1}{4}\left[t_1\left(x_1+\frac{1}{2}\right) - t_2\left(x_2+\frac{1}{2}\right)\right]\left(\rho_n\tau_n + \rho_p\tau_p\right) \\ &+ \frac{1}{16}\left[3t_1\left(1+\frac{1}{2}x_1\right) + t_2\left(1+\frac{1}{2}x_2\right)\right](\nabla\rho)^2 - \frac{1}{16}\left[3t_1\left(x_1+\frac{1}{2}\right) + t_2\left(x_2+\frac{1}{2}\right)\right]\left[\left(\nabla\rho_p\right)^2 + (\nabla\rho_n)^2\right] \\ &+ \frac{W_0^2}{4}\frac{2m}{\hbar^2}\left[\frac{\rho_p}{f_i}\left(2\nabla\rho_p + \nabla\rho_n\right)^2 + \frac{\rho_n}{f_i}\left(2\nabla\rho_n + \nabla\rho_p\right)^2\right] \end{aligned} \tag{10}$$

where t_0, t_1, t_2, t_3, x_0, x_1, x_2, x_3, and α are the Skyrme force parameters which are fitted by different authors to ground state properties of various nuclei. The last term in Eq. (10) describes the semi-classical expansion of spin-orbit densities up to second order in $\hbar^2$. The Coulomb energy density which includes direct and exchange contribution in Slater approximation can be written as

$$H_{\text{coul}}(r) = \frac{e^2}{2}\rho_p(r)\int\frac{\rho_p(r')}{|r-r'|}dr' - \frac{3e^2}{4}\left(\frac{3}{\pi}\right)^{\frac{1}{3}}\left(\rho_p(r)\right)^{\frac{4}{3}} \tag{11}$$

Using Eqs. (7)–(9), the total energy of nuclear system can be obtained in terms of neutron and proton densities under Skyrme interaction associated with ETF approximation [30–32]. Recently, Agrawal et al. [37] modified the Hamiltonian density (see Eq. (10)) on the following two accounts with six additional constants, two each for x_{3i}, t_{3i}, and α_1:

(i) The third term in Eq. (10) is replaced as

$$\frac{1}{2}\left[\sum_{\text{i}=1}^{3} t_{3\text{i}}\rho^{\alpha\text{i}}\left(1+\frac{1}{2}x_{3\text{i}}\right)\rho^2 - \left(x_{3\text{i}}+\frac{1}{2}\right)\left(\rho_{\text{n}}^2+\rho_{\text{p}}^2\right)\right] \tag{12}$$

(ii) A new term due to tensor coupling with spin and gradient is added as

$$-\frac{1}{16}\left(t_1x_1 + t_2x_2\right)\vec{\text{J}}^2 + \frac{1}{16}\left(t_1 - t_2\right)\left(\vec{\text{J}}_{\text{p}}^2 + \vec{\text{J}}_{\text{n}}^2\right) \tag{13}$$

The total Hamiltonian density given in Eq. (10) is the sum of the spin-orbit density-independent Hamiltonian density $H(\rho,\tau)$ and spin-orbit density-dependent Hamiltonian density $H\left(\rho,\vec{J}\right)$. In present work, we intend to calculate the nuclear interaction potential by employing different forces in SEDF approach to address the fusion excitation function data in the domain of the Coulomb barrier.

2.3 EDWSP Model

It will be discussed later in Sect. 3 that in the fusion of ${}^{32}_{16}S + {}^{94}_{40}Zr$ reaction, the use of different types of Skyrme interaction introduces similar kinds of barrier modification effects that arise from the coupled channel approach and the EDWSP model. The fusion dynamics of ${}^{32}_{16}S + {}^{94}_{40}Zr$ system is systematically analyzed further within the context of EDWSP model and coupled channel approach. In EDWSP model, the energy dependence in Woods-Saxon potential induces the various kinds of barrier modification effects and adequately addresses the fusion enhancement/fusion suppression in closely similar way as evident from the coupled channel formulation. The EDWSP model is used along with one-dimensional Wong formula, while the static Woods-Saxon potential is used within the view of the coupled channel approach. Therefore, the form of static Woods-Saxon potential is defined as

$$V_N(r) = \frac{-V_0}{\left[1+\exp\left(\frac{r-R_0}{a}\right)\right]} \tag{14}$$

with $R_0 = r_0\left(A_P^{\frac{1}{3}} + A_T^{\frac{1}{3}}\right)$. The "$V_0$" represents depth of potential, and "a" accounts for the diffuseness parameter of nuclear potential. In EDWSP model, the depth of real part of Woods-Saxon potential is defined as

$$V_0 = \left[A_P^{\frac{2}{3}} + A_T^{\frac{2}{3}} - (A_P+A_T)^{\frac{2}{3}}\right]\left[2.38 + 6.8(1+I_P+I_T)\frac{A_P^{\frac{1}{3}}A_T^{\frac{1}{3}}}{\left(A_P^{\frac{1}{3}}+A_T^{\frac{1}{3}}\right)}\right]\ \text{MeV} \tag{15}$$

where $I_P = \left(\frac{N_P - Z_P}{A_P}\right)$ and $I_T = \left(\frac{N_T - Z_T}{A_T}\right)$ are the isospin asymmetry of projectile and target nuclei, respectively. The EDWSP model includes the effects of the surface energy as well as the isospin asymmetry of colliding pairs [17–21]. The various channel coupling effects responsible for sub-barrier fusion enhancement are the surfacial effects, and during collisions, they modify the surface diffuseness as well as the surface energy of the collision partners and hence bring the requirement of larger diffuseness parameter to address the fusion excitation function data [1–3, 7–11, 16]. If a series of projectile is bombarded on a target isotope or vice versa, the isotopic dependencies of fusion excitation functions are directly reflected which must be incorporated in the theoretical description. In addition, all the nuclear structure effects like static and dynamical deformations and nucleon transfer channels are highly sensitive to surface region of nucleus-nucleus potential. These nuclear structure effects are directly linked with the diffuseness of Woods-Saxon potential and hence can be accommodated by variation of diffuseness parameter. Therefore, the EDWSP model takes care of all such static and dynamical aspects of heavy-ion collisions via energy-dependent diffuseness parameter. The energy-dependent diffuseness parameter is defined as

$$a(E) = 0.85\left[1 + \frac{r_0}{13.75\left(A_P^{\frac{1}{3}} + A_T^{\frac{1}{3}}\right)\left(1 + \exp\left(\frac{\frac{E}{V_{B0}} - 0.96}{0.03}\right)\right)}\right] fm \quad (16)$$

In theoretical calculations, this expression provides a wide range of diffuseness parameters depending upon the value of range parameter (r_0) and bombarding energy of colliding pairs. The range parameter r_0 is an adjustable parameter, and its values are optimized in order to vary the value of diffuseness of nuclear potential. From this article, one can say that the energy dependence in the nucleus-nucleus potential introduces the similar channel coupling effects that arise due to intrinsic degrees of freedom of collision partners. Furthermore, the variations of nucleon densities in the interior region of nucleus strongly depend upon the type of Skyrme force, while in the surface regions, the different kinds of Skyrme interactions lead to closely similar variations of nucleon densities [31–35]. It will be shown later that the theoretical calculations based upon SEDF and EDWSP model yield quite similar results in sub-barrier fusion dynamics, which clearly reveals that the various static and dynamical physical effects in the collision of heavy ion have strong impact in surface region only and such effects can be adequately incorporated by inducing the energy dependence in the nucleus-nucleus potential or alternatively by opting the appropriate Skyrme interaction.

2.4 Coupled Channel Model

Theoretically, the standard way to address the various channel coupling effects that arise due to coupling between relative motion and internal degrees of freedom of colliding nuclei is to solve the coupled channel equations. In theoretical calculations, it is very difficult to handle all the intrinsic channels but it is useful to include the dominant effects of relevant channels [38, 41, 42]. Therefore, the set of coupled channel equation can be written as

$$\left[\frac{-\hbar^2}{2\mu}\frac{d^2}{dr^2} + \frac{J(J+1)\hbar^2}{2\mu r^2} + V_N(r) + \frac{Z_P Z_T e^2}{r} + \varepsilon_n - E_{cm}\right]\psi_n(r) + \sum_m V_{nm}(r)\,\psi_m(r) = 0 \quad (17)$$

where $\overrightarrow{r}$ is the radial coordinate for the relative motion between fusing nuclei. μ is the reduced mass of the projectile and target system. The quantities E_{cm} and ε_n represent the bombarding energy in the center of mass frame and the excitation energy of the n^{th} channel, respectively. The $V_{n\,m}$ is the matrix elements of the coupling Hamiltonian, which in the collective model consists of Coulomb and nuclear components. For the coupled channel analysis, we used the code CCFULL [38], wherein the coupled channel equations are solved numerically by using the two basic approximations. The first approximation is no-Coriolis or rotating frame approximation which has been used in order to reduce the number of the coupled channel equations [38, 41, 42]. The second approximation, which is well applicable for the heavy-ion reactions, is the ingoing wave boundary conditions. According to IWBC, there are only incoming waves at the minimum position of the Coulomb pocket inside the barrier and there are only outgoing waves at infinity for all channels except the entrance channel. By including all the relevant channels, the total fusion cross section is defined as

$$\sigma_F(E) = \sum_J \sigma_J(E) = \frac{\pi}{k_0^2}\sum_J (2J+1)P_J(E) \quad (18)$$

where $P_J(E)$ is the total transmission coefficient corresponding to the angular momentum J. In the code CCFULL, the vibrational couplings in the harmonic limit are taken into account [38]. The operator in the nuclear coupling Hamiltonian for vibrational couplings is given by

$$\hat{O}_V = \frac{\beta_\lambda}{\sqrt{4\pi}} R_T\left(a_{\lambda 0}^{\dagger} + a_{\lambda 0}\right) \quad (19)$$

where R_T is parameterized as $r_{\text{coup}} A^{\frac{1}{3}}$, β_λ is the deformation parameter, and $a_{\lambda 0}^{\dagger}$ ($a_{\lambda 0}$) represents the creation (annihilation)

operator of the phonon of vibrational mode of multipolarity λ. In general, the nuclear coupling matrix elements are evaluated as

$$V_{nm}^{(N)} = \langle n|V_N\left(r, \hat{O}\right)|m\rangle - V_N^{(0)}\,\delta_{n,m}$$

The matrix elements of $\hat{O}_V$ between the n—phonon state $|n\rangle$ and the m—phonon state $|m\rangle$, which are needed for the vibrational coupling, is defined as

$$\hat{O}_{V(n\,m)} = \frac{\beta_\lambda}{\sqrt{4\pi}} R_T\left(\delta_{n,m-1}\sqrt{m} + \delta_{n,m+1}\sqrt{n}\right) \tag{20}$$

The Coulomb coupling matrix element for vibrational couplings is computed by the linear coupling approximation and is defined as

$$V_{V(n\,m)}^{(C)} = \frac{\beta_\lambda}{\sqrt{4\pi}} \frac{3}{2\lambda+1} Z_P Z_T e^2 \frac{R_T^\lambda}{r^{\lambda+1}} \times \left(\sqrt{m}\,\delta_{n,\,m-1} + \sqrt{n}\,\delta_{n,\,m+1}\right) \tag{21}$$

The total coupling matrix elements are obtained by taking the sum of $V_{nm}^{(N)}$ and $V_{nm}^{(C)}$.

3 Results and Discussion

This work systematically analyzed the fusion dynamics of ${}^{32}_{16}S + {}^{94}_{40}Zr$ reaction within the framework of the following three different approaches: role of different Skyrme forces within the one-dimensional Wong and ℓ-summed extended Wong formula, the static Woods-Saxon potential and the EWSDP model along with Wong formula, and the coupled channel approach wherein static Woods-Saxon potential is used to entertain the effects of intrinsic degrees of freedom of colliding pairs. In Wong and ℓ-summed extended Wong formula, the role of different Skyrme forces is tested to describe the sub-barrier dynamics of ${}^{32}_{16}S + {}^{94}_{40}Zr$ reaction within SEDF. The SEDF has advantage of using different Skyrme forces, which in turn lead to the different barrier characteristics (barrier height, barrier position, and barrier curvature). The details of calculations based upon different Skyrme forces are shown in Figs. 2 and 3. The barrier modification effects that arise due to use of different Skyrme forces in the fusion dynamics are shown in Fig. 1.

Here, the two Skyrme forces, namely, SIII and GSkI, are exploited for explaining the fusion enhancement of ${}^{32}_{16}S + {}^{94}_{40}Zr$ system. The reason for choosing SIII and GSkI forces among the available is that SIII is well-established old Skyrme force which has been successfully tested to address the fusion excitation function of many nuclear systems. On the other hand, GSkI is a new force which is parameterized by the experimental data on the bulk properties of nuclei ranging from normal to isospin-rich ones, and fitting procedure of GSkI requires three additional parameters. So in order to carry out the influence of the force parameter, we have opted one old established SIII force and another one latest having inclusion of isospin component and spin-orbit coupling, etc., i.e., GSkI force. Calculations have been done by using both spherical as well as deformed choices of colliding nuclei [43]. Barrier characteristics are main input in Wong model which get modified within inclusion of different Skyrme forces, thereby affecting the fusion probability and fusion excitation function across the barrier. In view of this, Fig. 1 is plotted, which shows the variation of total interaction potential $V_T(R)$ for two Skyrme forces SIII and GSkI by taking spherical as well as quadrupole deformed choices of colliding nuclei shown, respectively, in Fig. 1a, b. It is clear from graph that GSkI force has lower barrier height and larger barrier position as compared to SIII force. In other words, the barrier characteristics get modified within the change of Skyrme force. This kind of observed barrier modification is independent of deformation effects and in turn plays a significant role to address fusion enhancement at sub-barrier region as discussed in Figs. 2 and 3.

Figure 2 shows the variation of fusion cross section as a function of center of mass energy ($E_{c.\,m.}$) using Wong formula [24]. One can see that the fusion excitation functions calculated using SIII force within spherical choice of nuclei strongly underestimated the fusion data at below barrier energies and overestimate the data at above barrier energies. Although the inclusion of deformation effects slightly improve the results, still the experimental data could not be addressed. This discrepancy is due to non-inclusion of the isospin and spin-orbit coupling effects in SIII-based interaction. In other words, there is minor improvement particularly in below barrier region but still a significant variance is observed with respect to the experimental data. In order to incorporate the isospin and spin-orbit coupling effects, a new Skyrme force GSkI [37], which exhibits significantly different properties in comparison to SIII force, has been applied to explain the sub-barrier fusion dynamics of chosen reaction. Since GSkI force is obtained by fitting several properties of isospin-rich nuclei, so it is more appropriate for description of heavy-ion fusion reactions. It is clearly observed that GSkI reproduces experimental data at below barrier energy except at few energies in deep sub-barrier region whereas it still overestimates the fusion data at above barrier energies. Therefore, one may conclude that the use of GSkI force could address the below barrier fusion excitation functions quite adequately but at the expense of bad comparison at near and above barrier region. It is relevant to mention here that the use of different Skyrme forces enables us to have a variety of barrier characteristics and hence the addressal of fusion cross section gets significantly influenced due to barrier modification imparted. This barrier modification helps us to address the fusion enhancement/fusion hindrance somewhat similar to that of coupled channel approach.

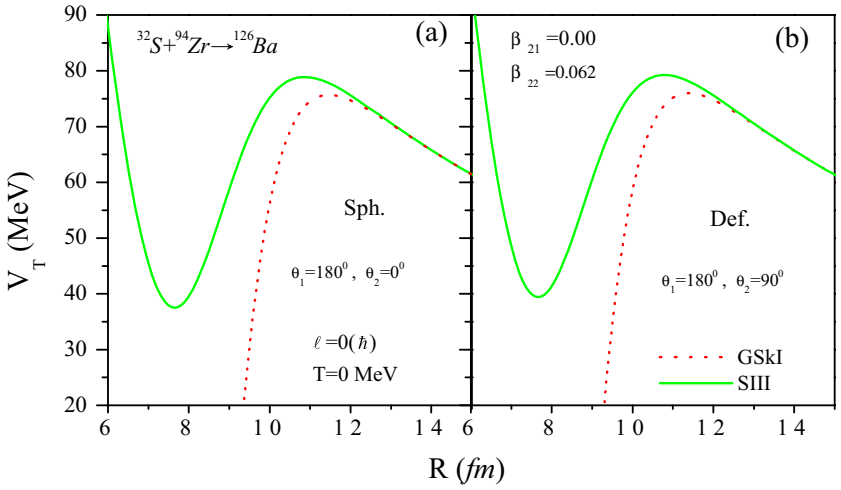

Fig. 1 Total interaction potential V_T(MeV) (**a** for spherical and **b** for deformed choices of colliding nuclei) as a function of inter nuclear separation R (*fm*)

In order to address the disagreement of fusion data in above barrier region, we have applied the ℓ-summed extended Wong formula with deformation effects included, and the same is depicted in Fig. 3. The prediction of ℓ-summed extended Wong formula within the context of SIII force is strongly suppressed by the experimental data. However, the GSkI force reasonably describes the fusion enhancement of this system at below barrier region. Also, the comparison improves significantly at above barrier region. It is important to note here that the barrier modifications, which mirror the variation of barrier characteristics that originate due to different Skyrme forces (SIII and GSkI), are responsible for the addressal of fusion enhancement at sub-barrier energies. Concludingly, in comparison to Wong formula, ℓ-summed extended Wong formalism takes care of overestimation at above barrier energies. In ℓ-summed extended Wong formula, we choose ℓ_{max} value empirically, while in simple Wong formula, ℓ dependence is taken from $\ell=0$ to ∞. Therefore, comparison improves across the barrier region for GSkI force as reported in Fig. 3.

After investigating the fusion excitation function of $^{32}_{16}S+^{94}_{40}Zr$ reaction in view of Wong and ℓ-summed Wong formalism within choices of different Skyrme interactions and analyzing the role of deformation effects of colliding nuclei, we intended to explore the fusion dynamics of chosen reaction in view of the static Woods-Saxon potential and the EDWSP

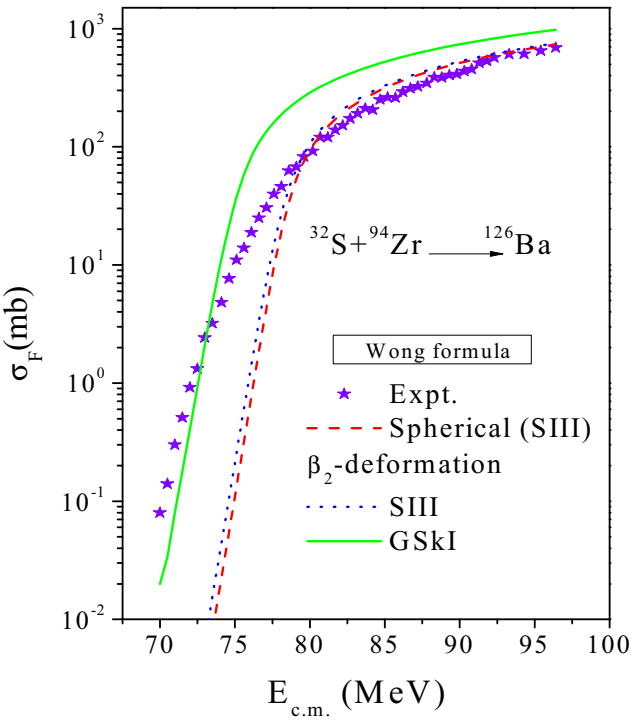

Fig. 2 The fusion excitation functions of $^{32}_{16}S+^{94}_{40}Zr$ system within the context of one-dimensional Wong formula using SIII and GSkI Skyrme forces are compared with the available experimental data [11]

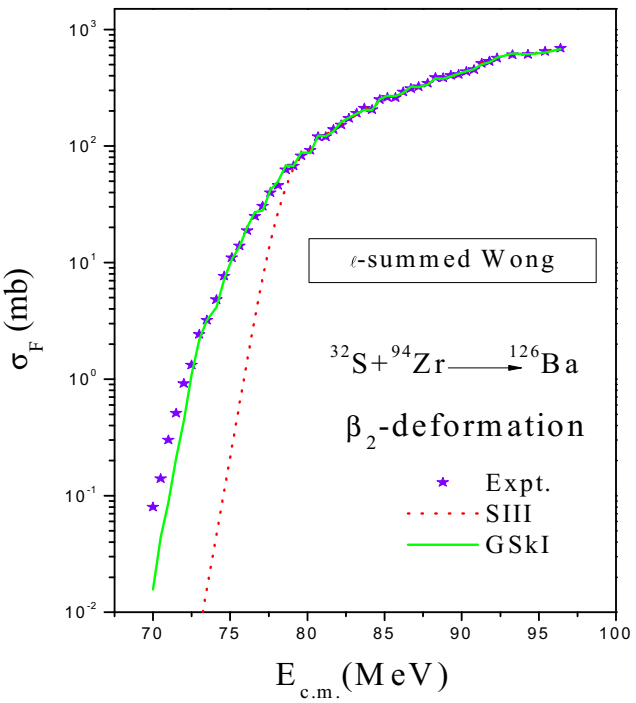

Fig. 3 Same as that of Fig. 2 but for ℓ-summed Wong formula

along with Wong formula. Theoretical predictions based upon the static Woods-Saxon potential along with Wong formalism are substantially underestimated by the experimental data of $^{32}_{16}S+^{94}_{40}Zr$ reaction, which clearly indicates that the static Woods-Saxon potential is not adequate to account the fusion enhancement of $^{32}_{16}S+^{94}_{40}Zr$ system. In the essence of giving single fusion barrier between fusing nuclei, the predictions of static Woods-Saxon potential in conjunction with Wong formula unable to address the observed fusion enhancement of this system as evident from Fig. 4.

However, the EDWSP model, wherein the energy-dependent diffuseness parameter induces spectrum of barriers of variable barrier heights, accurately describes the fusion enhancement of this system over a wide range of incident energies (see Fig. 5). The barrier height varies as a function of incident energy; henceforth, the different kinds of static and dynamical physical effects get automatically introduced in the theoretical calculations. All the entrance channel coupling effects like static and dynamical deformations and nucleon transfer channels are included via nucleus-nucleus potential. Therefore, the EDWSP model along with one-dimensional Wong formula provide much better description of sub-barrier fusion dynamics in comparison to simple Wong formula. Using Eq. (15), the value of depth parameter (V_0) comes out to be 95.45 MeV, while the range parameter ($r_0=1.118fm$) has been taken as free parameter to reproduce the experimental data. In EDWSP model calculations, $a=0.97fm$ is the largest value of diffuseness parameter which results in the lowest barrier ($FB=76.0$ MeV at $E_{c.m.}=68$ MeV and $a=0.97fm$ (see Fig. 5) and thus can be accounted for the shifting of maximum flux from relative motion to fusion channel. With the increase of incident energy, the value of diffuseness parameter decreases from $a=0.97fm$ to $a=0.85fm$, and consequently, the height of corresponding fusion barrier increases from $FB=76.0$ MeV to $FB=78.40$ MeV. This reduced barrier height (smaller than that of the Coulomb barrier) is in turn responsible to address the sub-barrier fusion enhancement. At above barrier energies, wherein fusion cross section is almost insensitive to the various channel coupling effects (internal structure of colliding nuclei), the value of diffuseness parameter gets saturated to its minimum value, and hence, largest fusion barrier is produced at this value of diffuseness parameter. The largest fusion barrier ($FB=78.40$ MeV at $E_{c.m.}=95$ MeV and $a=0.85fm$) produced in the EDWSP model calculations is still smaller than that of the Coulomb barrier (80.47 MeV). Therefore, in the EDWSP model, the lowering of fusion barrier between colliding nuclei can be ascribed for the prediction of larger sub-barrier fusion excitation function in comparison to that of static Woods-Saxon potential and hence adequately explain the observed fusion enhancement of $^{32}_{16}S+^{94}_{40}Zr$ reaction.

In addition to above, the effects of inelastic surface vibration of colliding nuclei on fusion dynamics of $^{32}_{16}S+^{94}_{40}Zr$ system are tested within the context of coupled channel calculations obtained by using code CCFULL. The $^{32}_{16}S$ nucleus is non-magic, while the $^{94}_{40}Zr$ nucleus is semi-magic nucleus, and both collision partners allow the low-lying inelastic surface vibrations as dominant mode of couplings. The deformation parameters of colliding nuclei as required for the coupled channel calculations are taken from ref. [11]. Quantitatively, no coupling calculations, wherein both collision partners are considered as inert, are unable to predict the required order of

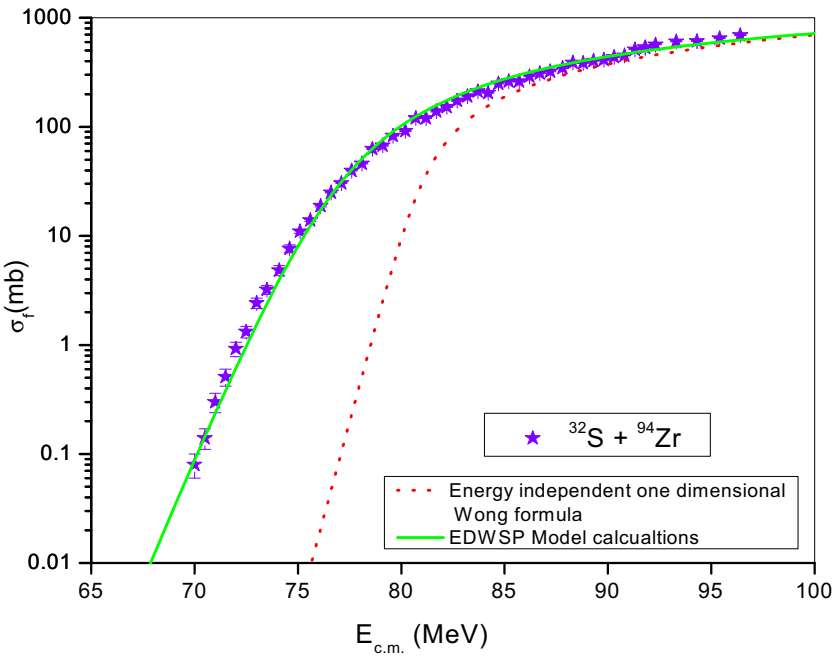

Fig. 4 We compare the fusion excitation function of $^{32}_{16}S+^{94}_{40}Zr$ system corresponding to the calculations performed by using the EDWSP model and static Woods-Saxon potential in conjunction with one-dimensional Wong formula. The theoretical calculations are compared with the available experimental data taken from [11]

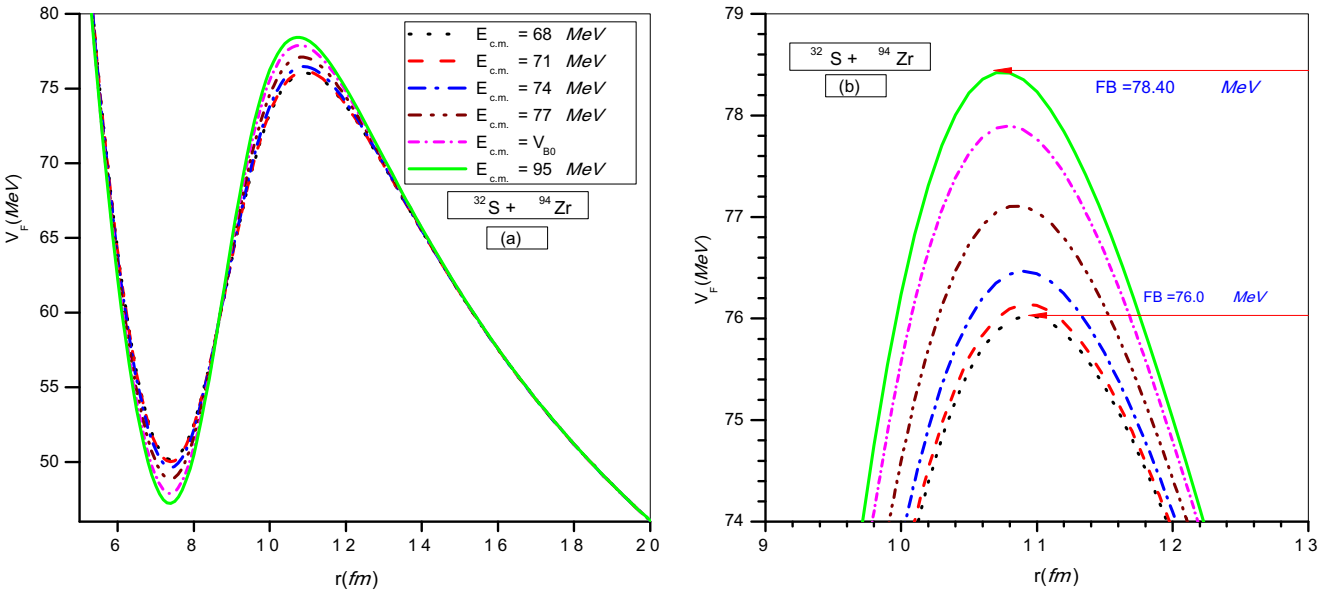

Fig. 5 The fusion barrier (FB) for $^{32}_{16}S + ^{94}_{40}Zr$ system obtained by using EDWSP model

magnitude of fusion enhancement at sub-barrier energies. The coupling to one-phonon 2^+ and 3^- vibrational states of colliding nuclei significantly enhances the magnitude of sub-barrier fusion excitation function with reference to no coupling case but fails to provide the close agreement with experimental data. This suggests the importance of coupling to higher multiphonon vibrational states. The inclusion of two-phonon vibrational states of type 2^+ and 3^- vibrational states along with their mutual coupling improve the results quantitatively, but more intrinsic channels are needed to account the observed fusion data. Although the coupling to low-lying 3^- vibrational state of target is expected to have strong impact on the fusion dynamics of this system, the sub-barrier fusion enhancement is almost insensitive to addition of higher multiphonon vibrational states such as three-phonon and four-phonon vibrational states as evident from Fig. 6.

Therefore, one may conclude that the theoretical predictions based upon static Woods-Saxon potential are substantially smaller than that of experimental data, whereas the predictions of the EDWSP model accurately describe the fusion dynamics of $^{32}_{16}S + ^{94}_{40}Zr$ system in whole range of energy and hence clearly mirror that the energy dependence in Woods-Saxon potential simulates various kinds of channel coupling effects occurring in the fusion dynamics of S-induced reaction

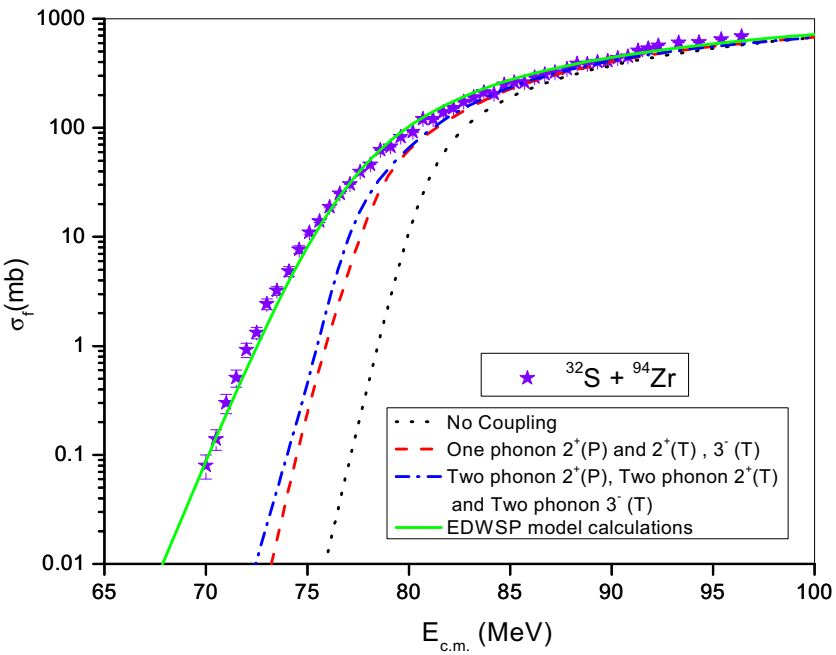

Fig. 6 Same as that of Fig. 4 but with coupled channel calculations and the EDWSP model. The theoretical calculations are compared with the available experimental data taken from [11]

(Fig. 6). The similar kinds of effects are introduced alternatively via use of different Skyrme forces within SEDF approach.

4 Conclusions

In the present work, we have analyzed the role of barrier modification effects introduced by the different theoretical approaches in the sub-barrier fusion dynamics of the $^{32}_{16}S+^{94}_{40}Zr$ system. The different Skyrme forces such as SIII and GSkI are used in the one-dimensional Wong and ℓ-summed extended Wong formula. In addition, the static Woods-Saxon potential and the EDWSP model are used in conjunction with the one-dimensional Wong formula. The effects of the intrinsic degrees of freedom of the colliding systems, such as inelastic surface excitations, are investigated by coupled channel calculations. It is observed that the predictions of the Wong formula with the static Woods-Saxon potential and SIII Skyrme force are substantially underestimated particularly in the sub-barrier region. The one-dimensional Wong formula with the GSkI force describes the fusion enhancement in the sub-barrier region but overestimates the data at above barrier energies. However, the ℓ-summed extended Wong formula with GSkI force reproduces the sub-barrier fusion data of the $^{32}_{16}S+^{94}_{40}Zr$ system quite adequately.

In consolidation of this, the role of low-lying surface vibrational states of the collision partners in the fusion of the $^{32}_{16}S+^{94}_{40}Zr$ system is tested within the context of the coupled channel approach, including only inelastic surface excitations. It fails to reproduce the fusion excitation function data at sub-barrier energies. This demands the addition of neutron transfer channels to account for the observed fusion enhancement. However, the predictions of the EDWSP model accurately describe the sub-barrier fusion enhancement of the $^{32}_{16}S+^{94}_{40}Zr$ system. In EDWSP-based calculations, the significantly larger diffuseness parameter ranging from $a=0.97fm$ to $a=0.85fm$ is required to describe the sub-barrier fusion data. Therefore, the present work suggested that the energy dependence in Woods-Saxon potential and the use of different Skyrme forces introduce similar kinds of barrier modification effects (barrier height, barrier position, and barrier curvature) as reflected from the coupled channel approach and hence provide adequate explanation of sub-barrier fusion enhancement of the $^{32}_{16}S+^{94}_{40}Zr$ system.

Acknowledgments This work was supported by UGC in the form of Dr. D. S. Kothari Post-Doctoral Fellowship Scheme and CSIR major research project, grant No:03(1341)/15/EMR-11.

References

1. L.F. Canto, P.R.S. Gomes, R. Donangelo, M.S. Hussein, Phys. Rep. **424**, 1 (2006)
2. K. Hagino, N. Takigawa, Prog. Theor. Phys. **128**, 1061 (2012)
3. B.B. Back, H. Esbensen, C.L. Jiang, K.E. Rehm, Rev. Mod. Phys. **86**, 317 (2014)
4. R.G. Stoksad et al., Phys. Rev. Lett. **41**, 465 (1978)
5. P.R.S. Gomes et al., Phys. Rev. C **49**, 245 (1994)
6. J.M.B. Shorto et al., Phys. Rev. C **81**, 044601 (2010)
7. H. Timmers et al., Nucl. Phys. A **633**, 421 (1998)
8. A.M. Stefanini et al., Phys. Rev. C **76**, 014610 (2007)
9. A.M. Stefanini et al., Phys. Rev. C **62**, 014601 (2000)
10. H.Q. Zhang et al., Phys. Rev. C **82**, 054609 (2010)
11. H.M. Jia et al., Phys. Rev. C **89**, 064605 (2014)
12. R.N. Sagaidak et al., Phys. Rev. C **76**, 034605 (2007)
13. N. Wang, W. Scheid, Phys. Rev. C **78**, 014607 (2008)
14. O.N. Ghodsi, R. Gharaei, Eur. Phys. J. A. **48**, 21 (2012)
15. D. Jain, R. Kumar, M.K. Sharma, Nucl. Phys. A **915**, 106 (2013)
16. J.O. Newton et al., Phys. Rev. C **70**, 024605 (2004)
17. M. Singh, Sukhvinder and R. Kharab, Nucl. Phys. A **897**, 179 (2013)
18. M.S. Gautam, Phys. Rev. C **90**, 024620 (2014)
19. M.S. Gautam, Nucl. Phys. A **933**, 272 (2015)
20. M.S. Gautam, Mod. Phys. Lett. A **30**, 1550013 (2015)
21. M.S. Gautam, Phys. Scr. **90**, 025301 (2015)
22. L.C. Chamon et al., Phys. Rev. C **66**, 014610 (2002)
23. K. Washiyama, D. Lacroix, Phys. Rev. C **74**, 024610 (2008)
24. C.Y. Wong, Phys. Rev. Lett. **31**, 766 (1973)
25. R. Kumar, M. Bansal, S.K. Arun, R.K. Gupta, Phys. Rev. C **80**, 034618 (2009)
26. R. Kumar, M.K. Sharma, R.K. Gupta, Nucl. Phys. A **870–871**, 42 (2011)
27. D. Jain, R. Kumar, M.K. Sharma, R.K. Gupta, Phys. Rev. C **85**, 024615 (2012)
28. D. Jain, R. Kumar, M.K. Sharma, Phys. Rev. C **87**, 044612 (2013)
29. M. Beiner, H. Flocard, N.V. Giai, P. Quentin, Nucl. Phys. A **238**, 29 (1976)
30. R.K. Puri, R.K. Gupta, Phys. Rev. C **51**, 1568 (1995)
31. D. Vautherin, D.M. Brink, Phys. Rev. C **5**, 626 (1972)
32. J. Bartel, K. Bencheikh, Eur. Phys. J. A **14**, 179 (2002)
33. M.K. Sharma, H. Kumar, R.K. Puri, R.K. Gupta, Phys. Rev. C **56**, 1175 (1997)
34. M.K. Sharma, R.K. Puri, R.K. Gupta, Eur. Phys. J. A **2**, 69 (1998)
35. D. Jain, M.K. Sharma, Rajni, R. Kumar, R.K. Gupta, Eur. Phys. J. A **50**, 155 (2014)
36. Rajni, R. Kumar, M.K. Sharma, Phys. Rev. C **90**, 044604 (2014)
37. B.K. Agrawal, S.K. Dhiman, K. Raj, Phys. Rev. **C 73**, 034319 (2006)
38. K. Hagino, N. Rowley, A.T. Kruppa, Comput. Phys. Commun. **123**, 143 (1999)
39. D.L. Hill, J.A. Wheeler, Phys. Rev. **89**, 1102 (1953)
40. M. Liu, N. Wang, Z. Li, X. Wu, E. Zhao, Nucl. Phys. A **768**, 80 (2006)
41. H. Esbensen, S. Landowne, C. Price, Phys. Rev. C **36**, 1216 (1987)
42. K. Hagino, N. Takigawa, A.B. Balantekin, J.R. Bennett, Phys. Rev. C **52**, 286 (1995)
43. P. Moller, J. R. Nix, W. D. Myers and W. J. Swiatecki, Atomic data and nuclear data tables **59**, 185 (1995)